ACS APPLIED MATERIALS & INTERFACES

Research Article

www.acsami.org

Significant Vertical Phase Separation in Solvent-Vapor-Annealed Poly(3,4-ethylenedioxythiophene):Poly(styrene sulfonate) Composite Films Leading to Better Conductivity and Work Function for High-Performance Indium Tin Oxide-Free Optoelectronics

Jun-Seok Yeo,[†] Jin-Mun Yun,[†,‡] Dong-Yu Kim,*[,†] Sungjun Park,[†] Seok-Soon Kim,[⊥] Myung-Han Yoon,[†] Tae-Wook Kim,[‡] and Seok-In Na*[,∥]

[†]School of Materials Science and Engineering, Gwangju Institute of Science and Technology, Gwangju 500-712, Republic of Korea

[‡]Korea Institute of Science and Technology (KIST), 864-9, Dunsan-ri, Bongdong-eup, Wanju-gun, Jeollabuk-do 565-902, Republic of Korea

[⊥]School of Materials Science and Chemical Engineering, Kunsan National University, Kunsan, Chonbuk 753-701, Republic of Korea

[∥]Graduate School of Flexible and Printable Electronics, Chonbuk National University, 664-14, Deokjin-dong, Jeonju-si, Jeollabuk-do, 561-756, Republic of Korea

ABSTRACT: In the present study, a novel polar-solvent vapor annealing (PSVA) was used to induce a significant structural rearrangement in poly(3,4-ethylenedioxythiophene):poly(styrene sulfonate) (PEDOT:PSS) films in order to improve their electrical conductivity and work function. The effects of polar-solvent vapor annealing on PEDOT:PSS were systematically compared with those of a conventional solvent additive method (SAM) and investigated in detail by analyzing the changes in conductivity, morphology, top and bottom surface composition, conformational PEDOT chains, and work function. The results confirmed that PSVA induces significant phase separation between excess PSS and PEDOT chains and a spontaneous formation of a highly enriched PSS layer on the top surface of the PEDOT:PSS polymer blend, which in turn leads to better 3-dimensional connections between the conducting PEDOT chains and higher work function. The resultant PSVA-treated PEDOT:PSS anode films exhibited a significantly enhanced conductivity of up to 1057 S cm^{-1} and a tunable high work function of up to 5.35 eV. The PSVA-treated PEDOT:PSS films were employed as transparent anodes in polymer light-emitting diodes (PLEDs) and polymer solar cells (PSCs). The cell performances of organic optoelectronic devices with the PSVA-treated PEDOT:PSS anodes were further improved due to the significant vertical phase separation and the self-organized PSS top surface in PSVA-treated PEDOT:PSS films, which can increase the anode conductivity and work function and allow the direct formation of a functional buffer layer between the active layer and the polymeric electrode. The results of the present study will allow better use and understanding of polymeric-blend materials and will further advance the realization of high-performance indium tin oxide (ITO)-free organic electronics.

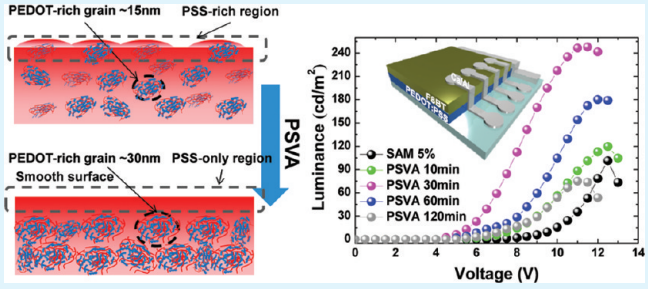

KEYWORDS: *PEDOT:PSS, phase separation, morphology, conductivity, work function, organic electronics*

INTRODUCTION

Flexible and printable organic-based optoelectronic devices have attracted significant interest due to their low-cost, flexibility, and lightweight properties.[1−3] The ultimate goal in this field is to realize high-efficiency, low-cost, and high-stability optoelectronic devices and to fabricate them cheaply and in large quantities by printing organic materials onto flexible substrates. However, current optoelectronic devices depend considerably upon indium tin oxide (ITO) transparent electrodes, although they possess inherent problems: the requirement of cost-intensive, high-temperature, and vacuum processes; an indium shortage due to the rapid development of touch screens and flat panel displays; and poor mechanical flexibility.[4,5] Hence, the absence of printable and flexible transparent electrodes has become a huge obstacle to realizing such electronic devices. To respond to this need, various ITO-alternative materials, such as conducting polymers,[5−7] metal wires,[8] carbon nanotubes,[9,10] and graphenes,[11,12] are being actively investigated as novel transparent electrodes for ITO-free printable and flexible optoelectronic devices.

Among various materials, highly conducting poly(3,4-ethylenedioxythiophene):poly(styrene sulfonate) (PE-

Received: February 10, 2012
Accepted: April 10, 2012
Published: April 10, 2012

DOT:PSS) has been regarded as a promising candidate for a next-generation printable and flexible transparent electrode for organic optoelectronic devices because of its solution processability, high transparency in the visible range, and high mechanical flexibility.[5,13,14] The currently accepted morphology of the PEDOT:PSS solid film is that it consists of PEDOT:PSS grains defined by high-molecular-weight PSS chains with PEDOT segments tightly and electrostatically attached along them and that the PEDOT:PSS grains are surrounded by neutral species, i.e., excess PSS, which fills the area between the polymer grains.[15−17] These PEDOT:PSS composites have generally been used as interfacial layers to improve hole injection or extraction in organic devices. Furthermore, with the aid of adding polar organic solvents or organic compounds such as dimethylsulfoxide (DMSO), *N*,*N*-dimethylformamide, and sorbitol into a PEDOT:PSS aqueous solution, the PEDOT:PSS was expended to be used as a transparent electrode in optoelectronic devices.[18−24] Currently, solvent-added PEDOT:PSS films have high conductivity of ∼700 S cm^{-1},[25,26] and the conductivity has increased up to 1418 S cm^{-1} after establishment of the two-step solvent-treatment method,[27] thus allowing fabrication of higher-performance ITO-free devices. However, although there are significant interests and efforts to use PEDOT:PSS as an electrode, there is a lack of in-depth observations and understanding about many features of solvent-treated PEDOT:PSS: the evolution of electronic and morphological properties with controlling processes; the origin of conductivity enhancement by solvent treatments; and the nature of charge transport in a solvent-treated PEDOT:PSS. More importantly, it remains a necessary challenge to improve the conductivity of PEDOT:PSS composites up to the ITO level or at least up to the amorphous ITO level, for the realization of full plastic and high-performance ITO-free optoelectronics.[5,28] Because PEDOT:PSS is a polymeric blend, the details of the processing conditions greatly affect the final film structure and morphology, which in turn can influence their macroscopic electrical properties.[18−20] Unfortunately, the spin-casted PEDOT:PSS films with conventional polar solvent treatments have limited drying time and morphological changes due to a rapid solvent quenching, and there exists a limitation to increase the amount of added polar solvents, since the increase in the amount of added polar solvent deteriorates the quality of film wetting.[29] Therefore, a novel method is critically needed to control the drying process with polar solvents for favorable morphology and enhanced conductivity of PEDOT:PSS films and to snapshoot direct evolution of various properties in a time scale for in-depth understanding of the solvent-treated PEDOT:PSS films.

In addition to the need to enhance the conductivity of PEDOT:PSS electrodes, modulating the work function of a transparent anode is also one of the most important factors to enhance device performance. It is well-known that the work function between the anode and the highest occupied molecular orbital (HOMO) of the organic material must be well matched in order to form an ohmic contact and to improve the charge injection and interface resistance, thereby enhancing cell performance.[30−32] Unfortunately, however, the work function (∼4.8−∼5.0 eV) of conventionally modified-PEDOT:PSS films in ITO-free organic devices is not high enough to match the energy levels of various organic active materials.[33−36] This can cause a large work-function mismatch between the PEDOT:PSS anode and the HOMO of the organic layer, which can adversely affect the charge injection or extraction in these devices. For these reasons, numerous modifications of electrodes by insertion of an interfacial layer have been intensively investigated in the effort to achieve high-performance organic devices.[30,37] However, to produce a promising interfacial layer for high-efficiency devices, various key factors such as transparency, conductivity, work function, film roughness, stability, wettability, and solution processability should be satisfied,[30,37,38] and the introduction of such interfacial layers into devices can result in a more complicated device structure and increased manufacturing costs.[36] Therefore, to use PEDOT:PSS electrodes for more promising printable and flexible transparent anodes, it would be highly desirable to develop a facile approach to achieve higher conductivity with no cost-intensive processes, higher work function without any electrode-interface tuning materials, or both.

Herein, we introduce a novel polar-solvent vapor annealing (PSVA) to induce a significant structural rearrangement in PEDOT:PSS-blend electrode films and to improve their electrical conductivity and work function. The effects of polar-solvent vapor annealing on PEDOT:PSS were investigated in detail by analyzing the changes in the conductivity, morphology, top and bottom surface composition, conformational PEDOT chains, and work function of the PSVA-treated PEDOT:PSS films, which was all systematically compared with those of a conventional solvent additive method (SAM). As a result, we found that the PSVA induced significant phase separation between excess PSS and PEDOT chains and the spontaneous formation of a highly enriched PSS layer on the top surface of the PEDOT:PSS polymer blend, which in turn led to better 3-dimensional connections between the conducting PEDOT chains and higher work function. The resultant PSVA-treated PEDOT:PSS anode films showed significantly enhanced conductivity up to 1057 S cm^{-1} and tunable high work function up to 5.35 eV. In addition, we also found that the introduction of the PSVA-treated PEDOT:PSS films as transparent anodes into organic optoelectronic devices such as polymer light-emitting diodes (PLEDs) and polymer solar cells (PSCs) further raised the device performance, mainly resulting from a significant vertical phase separation and a self-organized PSS top surface in the PSVA-treated PEDOT:PSS films that could increase the anode conductivity and work function and also allow the direct formation of a functional buffer layer between the active layer and the polymeric anode in the organic devices. This novel PSVA approach and the dual functionality of PSVA-treated PEDOT:PSS film to act simultaneously as a transparent electrode and as an interfacial buffer layer in devices will allow better use and understanding of polymeric blend systems and will further advance the realization of high-performance ITO-free organic electronics.

RESULTS AND DISCUSSION

In order to determine how polar solvent vapor annealing (PSVA) affects the electrical properties of PEDOT:PSS films, polymer films that were prepared with a pristine PEDOT:PSS aqueous solution (PH1000 from H. C. Starck) were fabricated using a time-dependent solvent annealing method with DMSO. The PSVA-treated PEDOT:PSS films were prepared as follows. A glass jar was prepared to conduct PSVA under a DSMO atmosphere by adding small amounts of DMSO (200 μL) into a covered glass jar and heating it at 150 °C for 1 min to vaporize the DMSO. The pure PEDOT:PSS was spin-coated at 1500 rpm onto a glass substrate and then directly transferred to

the prepared glass jar and kept in a wet film state under DMSO vapor for 1, 10, 30, 60, 120, 180, or 240 min. Immediately after vapor annealing, each film was thermally annealed at 150 °C for 30 min in ambient atmosphere to remove the residual solvent from the films.[19] For comparison, a reference PEDOT:PSS film was also fabricated using the solvent additive method (SAM), which was generally performed by adding various amounts of DMSO to the liquid PEDOT:PSS solution before film formation. The conventional SAM-treated PEDOT:PSS films were also prepared by spin-coating at 1500 rpm using formulated PEDOT:PSS solutions with various amounts of DMSO and were subsequently annealed at 150 °C for 30 min in an ambient atmosphere.

Figure 1 shows the conductivity of films modified with conventional SAM and PSVA, which was evaluated using 4-point-probe measurements. The pristine PEDOT:PSS films had low conductivity (~1 S cm^{-1}), and the conductivity was dramatically enhanced by adding DMSO. Above a DMSO concentration of 3%, the conductivity of the PEDOT:PSS films remained constant at around 700 S cm^{-1}. The highest conductivity of 820 S cm^{-1} and the average conductivity of 725 S cm^{-1} were obtained from the SAM-treated films with 5% DMSO. In the case of PEDOT:PSS films treated with the PSVA, the conductivity also increased with annealing time and then became saturated after solvent annealing for 30 min. However, beyond 180 min of PSVA, a dewetting phenomenon in the PSVA-treated PEDOT:PSS films resulted in an unreliable film.[39,40] As a result, a peak conductivity of 1057 S cm^{-1} and an averaged conductivity of 875 S cm^{-1} were obtained from the films that were treated by PSVA for 120 min. This value is comparable to the peak conductivity of 1024 S cm^{-1} obtained from the two-step treated PEDOT:PSS film that was repeated in our lab as recently reported by Kim et al.[27] Comparing the conductivities of these films with those of films with 5% DMSO, it was obvious that of the two treatment methods, PSVA was more effective as a means of enhancing the conductivity of PEDOT:PSS films, suggesting that the PSVA-treated PEDOT:PSS films could have a better PEDOT:PSS structure, distribution, or morphology for superior charge transport networks and better conducting connections in PEDOT:PSS complex films, compared with conventional SAM-treated PEDOT:PSS films.

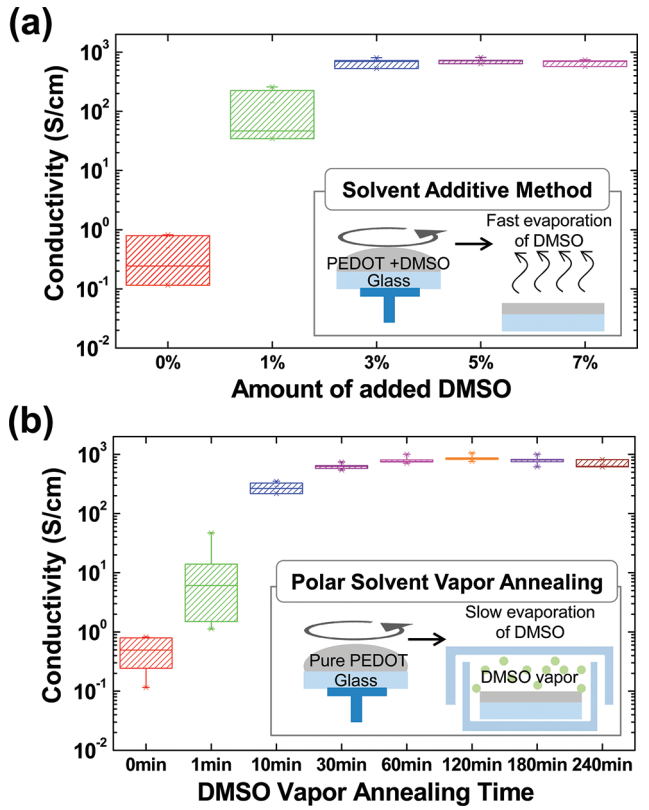

Figure 1. Conductivity of PEDOT:PSS composite films treated by (a) the SAM with various amount of added DMSO and (b) the PSVA with various times. Insets of (a) and (b): schematic illustrations of each treatment process.

To determine the origin of the enhanced conductivity of the PSVA-treated PEDOT:PSS, the morphologies of the pristine film, the SAM-treated film, and the PSVA-treated PEDOT:PSS film were first studied by atomic force microscopy (AFM), because the final film structure and morphology after completely evaporating the solvents are significantly dependent on the processing conditions, which in turn affects their macroscopic electrical properties.[18,41] Sample preparation for AFM measurement was the same as that used for 4-point-probe measurements, as shown in Figure 1. Figure 2a–e shows topographic images of the SAM-treated PEDOT:PSS films; the phase images are presented in the insets of Figure 2a–e. As the amount of added DMSO increased from 0 (pristine) to 7%, the surface root-mean-square (rms) roughness of the films gradually increased from 1.306 to 1.643 nm in the 1 × 1 μm^2 scan window. In the phase images, in which the PEDOT-rich (hard segments) and PSS-rich regions (soft segments) are shown as bright and dark regions, respectively,[19] the pristine PEDOT:PSS films showed 15–20 nm-sized PEDOT-rich grains. The size of the PEDOT-rich grains increased to about 30 nm as the concentration of DMSO increased from 0 to 3%, and there were no apparent changes in the grain size of films with a DMSO concentration higher than 3%. These morphological changes by the conventional SAM are consistent with the changes in conductivity shown in Figure 1a and in previous literature.[19,20] In contrast with the SAM-treated PEDOT:PSS films, by increasing the PSVA time from 0 (pristine) to 180 min, the surface rms roughness of the films was reduced substantially from 1.306 to 0.316 nm, as shown in Figure 2a,f–j. More interestingly, while the PEDOT-rich grains and PSS segments in the SAM-treated films were clearly revealed and distinguishable in the phase images, the image contrast in the phase image of the PSVA-treated films gradually became obscured, indicating that the top surface of the PSVA-treated PEDOT:PSS films consisted of a highly enriched component of either PEDOT or PSS.

In order to understand the apparently different behavior in the surface morphology of PEDOT:PSS films treated by either SAM or PSVA, we used X-ray photoemission spectroscopy (XPS) to study the surface chemical composition of the PEDOT:PSS films prepared by both polar solvent treatments. Because the sulfur atom in PEDOT is included in the thiophene ring, but in PSS it is within the sulfonate moiety, the S (sulfur) 2p spectra of PEDOT and PSS have different binding energies that allowed us to analyze the PEDOT:PSS composition.[20,42] Figure 3 shows the S 2p spectra of the PEDOT:PSS films treated with SAM and PSVA. The lower binding energy peaks at 164.5 and 165.6 eV and the higher binding energy peaks at 168.8 and 170.0 eV are associated with the PEDOT and PSS, respectively. The ratios of PEDOT-to-

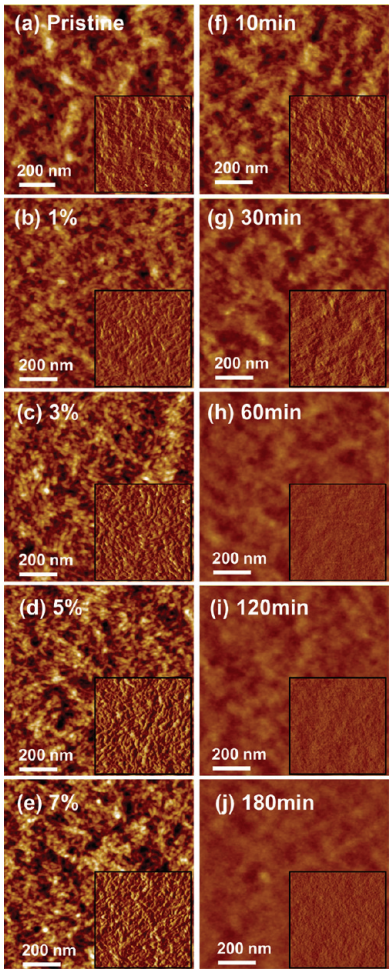

Figure 2. AFM topographic images of PEDOT:PSS composite films with different polar solvent treatments: SAM with (a) 0% (pristine), (b) 1%, (c) 3%, (d) 5%, and (e) 7%, and the PSVA during (f) 10 min, (g) 30 min, (h) 60 min, (i) 120 min, and (j) 180 min. All topographic images are in a vertical scale of 10 nm. The insets show the corresponding phase images with same date scale to topography, and all phase images are in a vertical scale of 5 degrees.

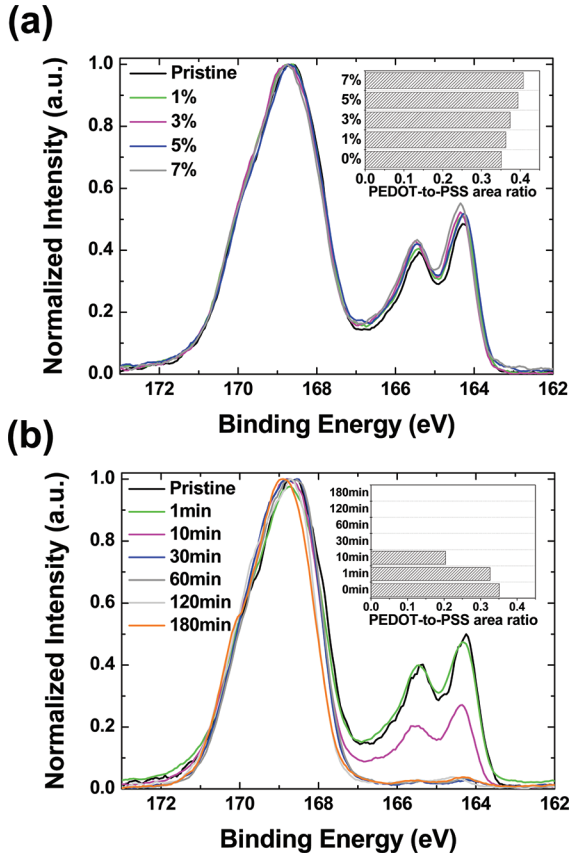

Figure 3. The S 2p spectra of PEDOT:PSS films modified with (a) SAM and (b) PSVA. Insets of (a) and (b): ratios of PEDOT-to-PSS at the surface of PEDOT:PSS films modified with polar solvent treatments.

PSS were calculated using the area ratio of the peaks assigned to PEDOT and PSS, and they are shown in the insets of Figure 3. It is well-known that the PSS composition at the top surface of PEDOT:PSS films is decreased by the addition of polar solvents.[17,20,33] In our experiment, the PEDOT-to-PSS ratio at the surface of the films also increased as the amount of added DMSO increased, indicating that the surface PEDOT-to-PSS ratios of the SAM-modified PEDOT:PSS films approached the bulk PEDOT-to-PSS ratio as the amount of added DMSO was increased. These surface-compositional changes in the XPS data shown in Figure 3a were well matched to morphological changes such as the enlarged PEDOT-rich grains shown in Figure 2a–e. Because how well charges are transported among the highly conducting PEDOT-rich grains will decide the overall conductivity of PEDOT:PSS films, the enlarged PEDOT-rich grains, resulting in thinner PSS barriers, will currently be the most accepted reason for enhanced conductivity in the PEDOT:PSS films modified by conventional polar solvent treatments.[18−20] Interestingly, however, we could see that quite different changes occurred when the PEDOT:PSS films were annealed with PSVA; the PSS component became enriched at the surface of the PEDOT:PSS films, as shown in Figure 3b. The PEDOT-to-PSS ratios of the PSVA-treated PEDOT:PSS films were sharply reduced, and the peaks corresponding to PEDOT began to disappear after 30 min of PSVA, indicating that the PSS was segregated to the top surface of the films. From these results, it is believed that the PSVA can induce a significant vertical phase separation between excess PSS and PEDOT chains, thus resulting in the formation of a highly enriched PSS layer on the top surface. This will be considered a novel result that a highly enriched PSS layer, formed on the top surface in solvent-modified PEDOT:PSS electrode films, can be induced and controlled with a solvent-treatment approach.

Because the highly enriched PSS top layer on the PSVA-treated films obscured the underlying bulk morphology and composition of the films, we could find no evidence of more enhanced conductivity in the PSVA-treated PEDOT:PSS films, compared with the SAM-treated films. Therefore, to determine the mechanism for the conductivity enhancement in the PSVA system, we investigated the Raman spectra of the PSVA-treated and the conventional SAM-treated PEDOT:PSS films. The conformational changes of the PEDOT chains in the PEDOT:PSS films caused by the polar solvent treatments can be studied in the Raman spectra of the films. Quyang et al. reported that the conformational changes of the PEDOT chains from benzoid to quinoid structure increased interchain interaction, thereby enhancing the conductivity of the solvent-treated PEDOT:PSS films.[21,22] As shown in Figure 4a,b, in both the PSVA and the SAM cases, the shoulder signals

dx.doi.org/10.1021/am300231v | ACS Appl. Mater. Interfaces 2012, 4, 2551−2560

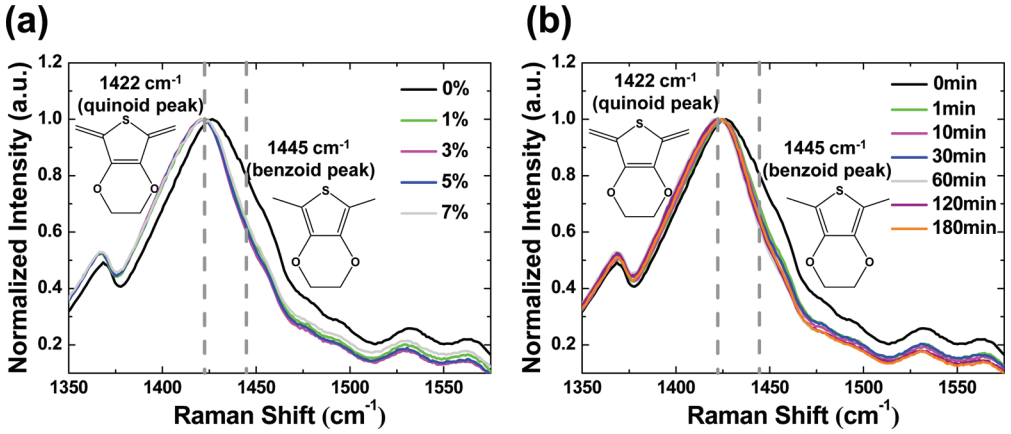

Figure 4. Raman spectra of PEDOT:PSS composite films treated with (a) SAM and (b) PSVA recorded at an excitation wavelength of 632.8 nm.

at 1445 cm^{-1} corresponding to a benzoid structure became weaker relative to the pristine PEDOT:PSS film after polar solvent treatments, indicating that the benzoid structure was converted to the quinoid structure so as to be more favorable to inter- and intrachain charge transport in PEDOT. However, although the variation of their conductivity between the 1 min (or 1%) and 120 min (or 5%) samples was large as shown in Figure 1, the relative intensity of the benzoid structure to the quinoid structure in the Raman spectra was not apparently varied after an 1 min PSVA (or 1% SAM) treatment. These results suggested that the continuous conductivity enhancement beyond the 1 min-PSVA-treated (or the 1%-SAM-treated) PEDOT:PSS films could not be fully explained even by the conformational change of the PEDOT chains in the bulk films to obtain the Raman spectra shown in Figure 4.

To better investigate the main factor affecting the further enhanced conductivity of films grown by PSVA, we evaluated electrical transport properties of solvent-modified PEDOT:PSS films in the parallel and perpendicular directions, as shown in Figure 5. Nardes et al. previously demonstrated that the dc conductivities measured in the lateral and vertical directions of pristine PEDOT:PSS films are highly correlated with the morphology observed using cross-sectional AFM.[15] Therefore, such investigation on lateral and vertical conductivity could be one of the most direct experimental approaches to study and explain morphological and charge-transport changes that occur throughout the entire PSVA-treated film. To investigate the in-plane and out-of-plane electrical properties, devices with different electrode geometries were designed, as shown in the insets of Figure 5a,b. As shown in Figure 5a, dc conductivity measured in the lateral direction presented a behavior similar to the conductivity changes shown in Figure 1, and the PSVA-treated films showed slightly increased lateral conductivity compared with those of SAM-treated films. Furthermore, as shown in Figure 5b, unlike the vertical conductivity of the SAM-treated PEDOT:PSS films showing saturated behavior at DMSO concentrations of 1% or greater, the vertical conductivity of the PSVA films gradually increased with PSVA time to 120 min, and the vertical conductivity of the 120 min-PSVA-treated film was approximately two times higher than the best conductivity of the conventional SAM-treated film. These results well support that compared with conventional SAM-treated films, PSVA induces a significant 3-dimensional (3-D) structural rearrangement in PEDOT:PSS blend films and produces a more noticeable vertical phase separation between excess PSS and PEDOT chains, which in

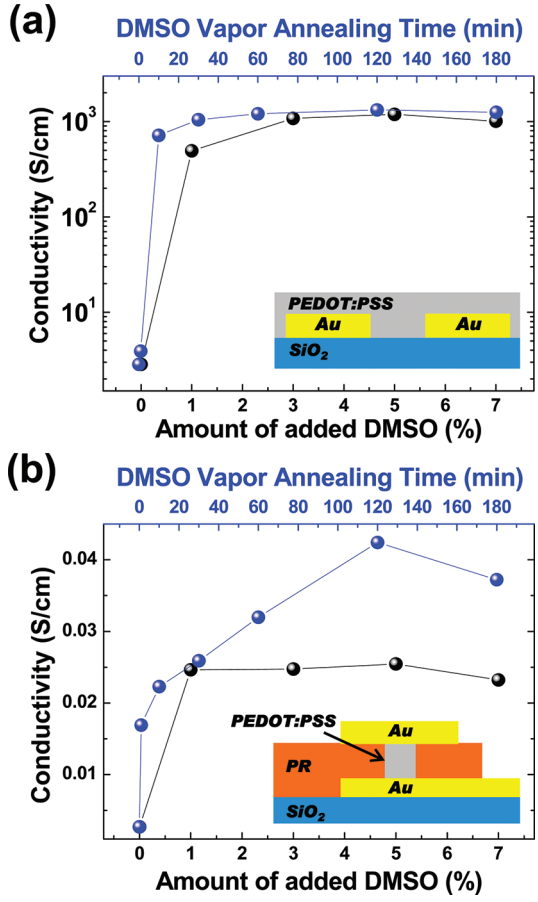

Figure 5. Changes in lateral and vertical dc conductivity of PEDOT:PSS films modified by both polar solvent treatments: the conductivities measured (a) in parallel to the substrate and measured (b) in perpendicular to the substrate as functions of various concentrations of SAM and PSVA times. Insets of (a) and (b) show the schematic structures of the devices fabricated for the in-plane and out-of-plane dc conductivity measurements.

turn leads to the spontaneous formation of a highly enriched PSS layer on the top surface and better 3-dimensional connections between the conducting PEDOT chains, thereby increasing the conductivity.

To strengthen the aforementioned results and interpretation, we carried out a morphological investigation of the buried bottom surface of PEDOT:PSS films using a lift-off

dx.doi.org/10.1021/am300231v | ACS Appl. Mater. Interfaces 2012, 4, 2551−2560

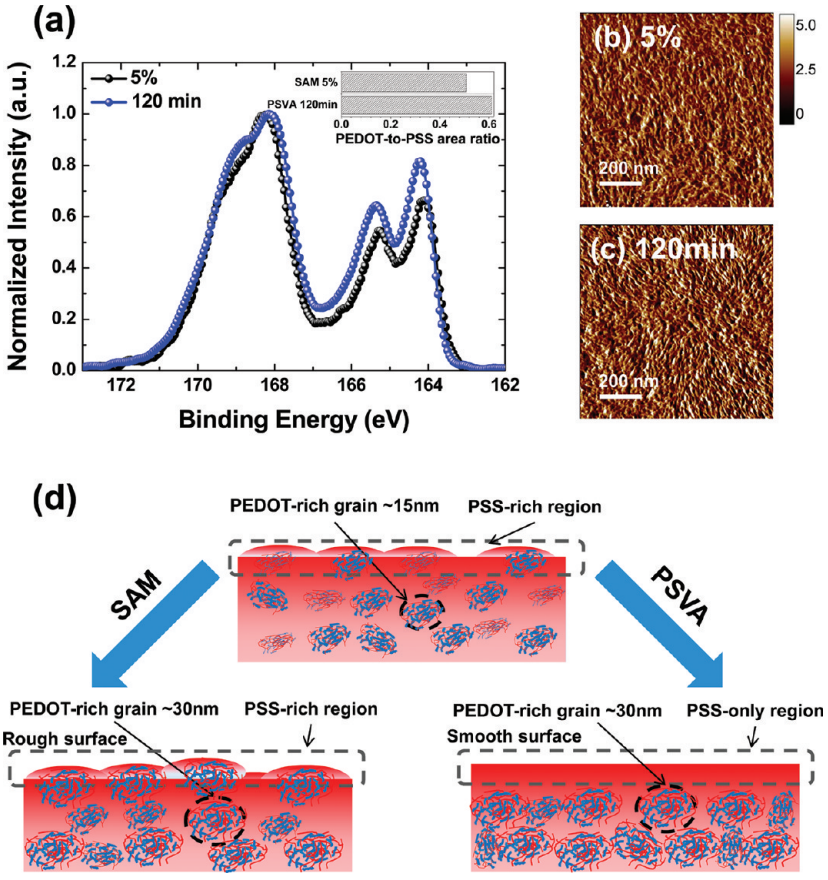

Figure 6. (a) XPS spectra of S 2p at the bottom surface of PEDOT:PSS films treated with SAM of 5% and PSVA for 120 min. Phase images of PEDOT:PSS films modified by (b) SAM of 5% and (c) PSVA for 120 min. (d) The schematic morphological models of spin-coated pristine, SAM-treated, and PSVA-treated PEDOT:PSS films. Inset of (a) shows the ratio of PEDOT-to-PSS at the bottom surface of the modified PEDOT:PSS films.

method,[43,44] and the bottom surfaces were characterized with XPS and AFM. The details of the lift-off method are described in the Experimental Section. Figure 6a shows the S 2p spectra obtained from the bottom side of PEDOT:PSS films. In the case of the 120 min-PSVA-treated film, the intensity of the lower binding energy peaks at around 165 eV corresponding to PEDOT were higher than the SAM 5%-treated film, which indicated that the PEDOT contents in the bottom surface of the 120 min-PSVA-treated films were more concentrated compared with the SAM 5%-treated films. As shown in the inset of Figure 6a, the PEDOT-to-PSS ratios at the bottom surface were increased from 0.51 to 0.61 by replacing the SAM with the PSVA. Furthermore, as observed in the AFM phase images of Figure 6b,c, the bottom surface of the PSVA-treated film showed more densely distributed PEDOT-rich grains and better connections between the bright PEDOT-rich regions compared with those of the conventional SAM-treated film. These morphological changes in the AFM bottom surface will be well correlated with the bottom-surface compositional changes in XPS. More importantly, these results strongly support that the PSVA-treated PEDOT:PSS electrode has a significant composition gradient from the surface to the bulk of the film and the self-organized PSS-enriched layer at the top surface of the blend film.

These significant 3-D morphological changes, outstanding vertical phase separation, and conductivity changes in the PSVA-treated PEDOT:PSS can be explained by the following factors. As is well-known, it is highly important to increase the remaining time and amount of polar solvent in PEDOT:PSS films in order to obtain higher conductivity of PEDOT:PSS films, because the phase separation and morphological changes of PEDOT:PSS occur mainly until the polar solvent and water are completely evaporated, and they greatly affect the charge transport and conductivity in films.[18−20] In addition, because the polar solvents lower the interaction between the PEDOT-rich core and excess PSS, the weakened interactions between them enable excess PSS to migrate easily in a thermodynamically favorable direction, which results in a continuous phase separation until completely evaporating the water and polar solvents.[20,45,46] However, the spin-coated PEDOT:PSS films treated with the conventional SAM would have limited conductivity and 3-D morphology, because the use of a spin-coating process can remove extensive amounts of the water and polar solvent and can accelerate the drying time of the film,[47] and the film-wetting property can be worsened with the addition of polar solvents,[29] inevitably preventing it from reaching a morphology with more equilibrium.[47,48] In contrast, when PEDOT:PSS films are treated with PSVA, 3-D morphological changes, vertical phase separation, and conductivity changes will be more activated, because the PEDOT:PSS films can be exposed to more highly concentrated polar solvents for longer times to diffuse excess PSS as demonstrated by the AFM, XPS, and conductivity data. Therefore, the schematically morphological images of the pristine PEDOT:PSS, the conventional SAM-treated PEDOT:PSS, and the PSVA-treated PEDOT:PSS could be

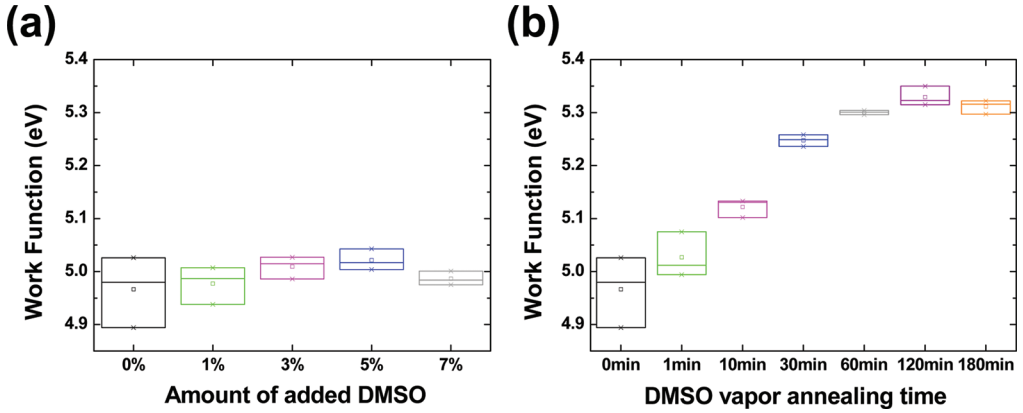

Figure 7. Variation of work function in PEDOT:PSS films modified with (a) various concentration of SAM and (b) various times of PSVA.

drawn as Figure 6d. We believe that taken together, the results in Figures 1–6 show that the PSVA induced a significant composition gradient and a spontaneous formation of a highly enriched PSS layer on the top surface of the blend film, providing better 3-D connections between the conducting PEDOT chains and greater depletion of the insulating PSS barriers between the PEDOT regions, inevitably increasing anode conductivity.

In addition to the conductivity of a transparent anode, the work function of an anode also plays a critical role in determining the performance of the device because the energy level difference between the anode and the active organic layer acts as a hole injection or extraction barrier.[30−32,36] In this respect, prior to direct application to optoelectronic devices, we measured the work function of PEDOT:PSS films as a function of the amount of added DMSO and the PSVA time as shown in Figure 7a,b, respectively. The work function measurements were carried out using ultraviolet photoelectron spectroscopy (UPS). The results for PEDOT:PSS films treated by SAM were in the range of 4.99 ± 0.02 eV for different amounts of added DMSO, which showed that the work function did not vary greatly with DMSO concentration. However, in the case of the PSVA system, the work function of PEDOT:PSS films was systematically tuned with annealing time. Figure 7b shows that the work function of PEDOT:PSS with the PSVA system gradually increased with annealing time but leveled off in the range of 5.30 ± 0.05 eV after the 30 min of annealing time. The correlation of the top surface composition in Figure 3 with the work function shows that the tunable work function of PEDOT:PSS films stems from the enriched PSS at the surface because the concentrated PSS at the film surface could lead to a decrease in the density of filled states near the Fermi level.[32] Eventually, it was confirmed that with the PSVA approach, in addition to achieving higher conductivity, higher work function (5.35 eV) of PEDOT:PSS anodes can be obtained with no electrode-interface tuning materials and no cost-intensive processes. More importantly, the above results confirm that the significant vertical phase separation and the self-organized PSS top surface in PSVA-treated PEDOT:PSS films can increase the anode work function and conductivity and in particular can also allow the direct formation of a functional buffer layer between the active layer and the polymeric anode in the organic devices to decrease interface resistances and improve cell performance.[30,31,49]

To evaluate directly the potentials of the PSVA-treated PEDOT:PSS films as transparent anodes for ITO-free optoelectronic devices, we first fabricated polymer light-emitting diodes (PLEDs) using a PSVA-treated PEDOT:PSS anode and compared our results to a device based on a conventional SAM-treated PEDOT:PSS anode. Figure 8a presents the luminance characteristics of PLEDs based on PEDOT:PSS anodes and the energy level positions of each component. A commercially available poly(9,9-dioctylifluorene-co-benzothiadiazole) (F8BT) as an emissive layer was coated onto each polymeric anode; a detailed configuration of the PLEDs in this experiment is shown in the inset of Figure 8a. As shown in Figure 8a and Table 1, compared with the devices with SAM-5% treated PEDOT anodes (7.50 V and 101.3 Cd

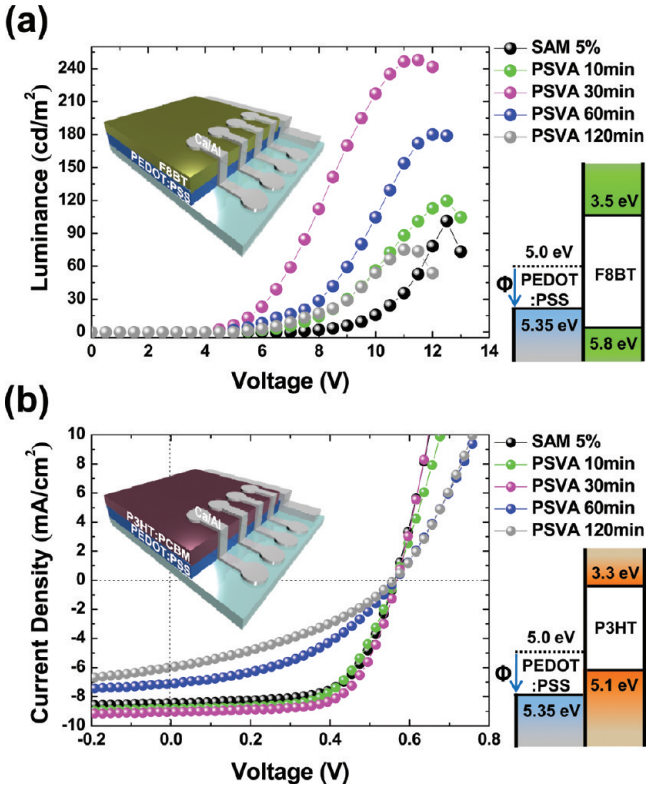

Figure 8. (a) Luminance characteristics of PLEDs and (b) *J*–*V* characteristics of PSCs with PSVA-treated PEDOT:PSS anodes and a 5% SAM-treated PEDOT:PSS anode for reference containing the corresponding energy diagrams. Insets of (a) and (b) show the device structures of PLEDs and PSCs.

Table 1. Summary of Device Characteristics for PLEDs and PSCs Based on PSVA-Treated PEDOT:PSS Anodes and 5% SAM-Treated PEDOT:PSS Film for a Reference Anode

PLEDs	turn-on voltage (V)	maximum luminance (Cd m^{-2})
5%	7.5	101.3
10 min	5.50	119.7
30 min	4.50	247.9
60 min	5.00	180.0
120 min	5.5	75.11

PSCs	FF	J_{sc} (mA cm^{-2})	V_{oc} (V)	PCE (%)	R_s (Ω cm^2)	R_{sh} (MΩ cm^2)
5%	0.622	8.68	0.561	3.01	4.77	0.08
10 min	0.602	8.84	0.561	2.95	8.03	2.16
30 min	0.651	9.16	0.560	3.35	4.10	1.37
60 min	0.431	7.32	0.565	1.78	12.3	3.38
120 min	0.363	5.80	0.563	1.19	15.7	3.22

m^{-2}), the turn-on voltages and the maximum luminance of the cells with the PSVA-treated PEDOT:PSS films were all improved except for the maximum luminance of the cell with the 120 min-PSVA-treated PEDOT anode: 5.50 V and 119.7 Cd m^{-2} at 10 min, 4.50 V and 247.9 Cd m^{-2} at 30 min, 5.00 V and 180.0 Cd m^{-2} at 60 min, and 5.50 V and 75.11 Cd m^{-2} at 120 min. Considering that all materials and processes used to fabricate the PLEDs were identical except for the polar-solvent treatment method for PEDOT:PSS electrodes and that the device performance of the ITO-free optoelectronic devices were generally related closely to the work function and conductivity of the transparent electrode, the reduced turn-on voltages and the enhanced luminescence in PSVA-treated PEDOT-based cells are believed to arise from the significant vertical phase separation and the self-organized PSS top surface in the PSVA-treated PEDOT:PSS films to improve the anode work function and conductivity, thus enhancing the charge injection, internal resistance, and cell performance.[30−32,50] However, as shown in Figure 8a, although the PEDOT:PSS electrodes that were PSVA-treated for more than 30 min showed somewhat more favorable conductivity and work function, the devices with 60 min and 120 min-treated PEDOT anodes exhibited increased turn-on voltages (5.0 and 5.5 V, respectively) and decreased maximum luminance (180.0 and 75.11 Cd m^{-2}, respectively) compared to those with 30 min-PSVA-treated PEDOT anodes. This performance degradation in PLEDs with PEDOT anodes that were PSVA-treated beyond 30 min could be due to the thickness of the self-organized PSS insulating layer being thicker than the tunneling range with increasing PSVA times, which can increase the internal resistance.[51] More importantly, the overall enhanced cell performances in the PSVA-treated, PEDOT-based PLEDs clearly demonstrated that PSVA-treated PEDOT:PSS is better suited than conventional SAM-based PEDOT:PSS for fabrication of more efficient ITO-free PLEDs.

To further expand the potential of PSVA-treated, dual functional PEDOT:PSS films in organic optoelectronics, we also examined the performance of polymer solar cells (PSCs) based on poly(3-hexylthiophene) (P3HT) and 1-(3-methoxycarbonyl)-propyl-1-phenyl-(6,6)C_{61} (PCBM) bulk-heterojunction (BHJ) systems as shown in Figure 8b. The representative photovoltaic characteristics under 100 mW cm^{-2} illumination with an AM 1.5 G condition and the series resistances (R_s) and shunt resistances (R_{sh}) calculated from the dark current density−voltage ($J-V$) curves of PSCs are summarized in Table 1. As demonstrated in Figure 8b, power conversion efficiency (PCE) values in cells with PEDOT:PSS films modified by PSVA increased with PSVA times of up to 30 min but became degraded when the PSVA time was extended further: 2.95% at 10 min, 3.35% at 30 min, 1.78% at 60 min, and 1.19% at 120 min. The PSC with the 30 min-PSVA-treated PEDOT:PSS film exhibited the best photovoltaic performance as follows: short-circuit current (J_{sc}), 9.16 mA cm^{-2}; open-circuit voltage (V_{oc}), 0.560 V; fill factor (FF), 0.651; and power conversion efficiency (PCE), 3.35%. In contrast, FF of 0.622, J_{sc} of 8.68 mA cm^{-2}, V_{oc} of 0.561 V, and PCE of 3.01% were obtained from the reference cell with the SAM 5%-treated PEDOT anode. Compared to the cell with the 5% SAM, it was clear that most of the increase in PCE of the cell with the 30 min PSVA originated from FF and J_{sc} rather than V_{oc}. In PSCs, although the work function of PEDOT-anode was increased up to ∼0.35 eV with the PSVA treatment, the value of the work function did not influence the value of V_{oc} because the work function of the PEDOT anode, even under SAM 5%, was high enough to form an ohmic contact with P3HT. Unlike the independence of V_{oc} on the polar-solvent treatment type, the values of FF and J_{sc} were enhanced by replacing 5%-SAM-treated PEDOT:PSS anodes with 30 min-PSVA-treated PEDOT:PSS anodes. In general, the FF and J_{sc} are closely linked to R_s and R_{sh}. For better comparative studies, we calculated both R_s and R_{sh} from the $J-V$ curves of solar cells in dark conditions. As shown in Table 1, compared with R_s (4.77 Ω cm^2) and R_{sh} (0.08 MΩ cm^2) of the SAM-treated sample, the PSC with the 30 min-PSVA-treated PEDOT anode showed a better R_s (4.10 Ω cm^2) and, in particular, presented a much higher R_{sh} (1.37 MΩ cm^2). This indicates that the self-organized PSS top layer in PSVA-treated PEDOT anodes, having an insulating property and a smooth surface, can better protect the BHJ active layer from directly contacting the highly conducting and rough PEDOT-rich grains and can form a better uniform contact between the active layer and the PEDOT anode compared with the conventional solvent-modified PEDOT anode having a relatively more conductive and rougher PEDOT-rich top surface, consequently improving the overall resistance and cell performance of the PSCs.[38,49,52] More importantly, the results shown in Figure 8a,b demonstrate that compared with conventionally treated PEDOT:PSS, the PSVA-treated PEDOT:PSS electrode with greater conductivity, higher work function, and a dual-function to act simultaneously as a transparent electrode and as an interfacial layer in devices is a more promising candidate for further advancing the realization of better performance ITO-free organic electronics. It should also be noted that with the novel PSVA approach, it is possible to achieve a dual-function PEDOT:PSS electrode to act simultaneously as a transparent electrode and as a functional interfacial layer in optoelectronic devices.

CONCLUSIONS

In conclusion, a novel polar-solvent vapor annealing (PSVA) to induce a significant structural rearrangement in PEDOT:PSS blend films and also to improve the electrical conductivity and work function of PEDOT:PSS electrode films was studied in detail. To better understand the effects of polar-solvent vapor annealing on PEDOT:PSS, changes in the conductivity, morphology, top and bottom surface composition, conformational PEDOT chains, and work function of the PSVA-treated PEDOT:PSS films were all systematically investigated and

compared with films produced by the conventional solvent additive method. The results clearly confirmed that the PSVA induced significant phase separation between excess PSS and PEDOT chains and the spontaneous formation of a highly enriched PSS layer on the top surface of the PEDOT:PSS polymer blend, which in turn led to better 3-dimensional connections between the conducting PEDOT chains and higher work function due to the self-organized PSS layer on top of the polymeric anode films. As a result, the PSVA-treated PEDOT:PSS anode films exhibited significantly enhanced conductivity up to 1057 S cm^{-1} and tunable high work function up to 5.35 eV. To the best of our knowledge, this work is the first report regarding solvent-treated PEDOT:PSS anode films with a significant vertical phase separation and self-organized PSS top surface to simultaneously increase anode conductivity and work function. In addition, it should also be noted that the device performance of PLEDs and PSCs with PSVA-treated PEDOT:PSS anode films were further improved due to the significant vertical phase separation and the spontaneously formed PSS top surface in the PSVA-treated PEDOT:PSS films that increased the anode conductivity and work function and allowed the direct formation of a functional buffer layer between the active layer and the polymeric anode in organic devices. These results clearly demonstrate that the novel PSVA approach and the dual functionality of PSVA-treated PEDOT:PSS film to act simultaneously as a transparent electrode and as an interfacial buffer layer in devices are promising candidates for further advancing the realization of better-quality polymeric-blend films and better-performing ITO-free organic electronics.

EXPERIMENTAL SECTION

Preparation of PEDOT:PSS Films. The glass substrates (Eagle 2000, Corning) were cleaned with ultrasonic treatment in both acetone and isopropyl alcohol, and the cleaned substrates were then treated with UV/ozone for 30 min before deposition of PEDOT:PSS. PH 1000 (Clevios PH 1000 from by H. C. Starck) and DMSO-added PH 1000 aqueous solutions were spin-coated onto the cleaned glass substrates at 1500 rpm for 40 s using a 0.45 μm hydrophilic filter. For PEDOT:PSS films fabricated by PSVA, spin-coated PEDOT:PSS films using the pristine PH 1000 solution were kept in a wet film state under DMSO vapor in a capped glass jar (5 cm in diameter by 1 cm in height) for various times. All the PEDOT:PSS films after polar solvent treatments were subsequently dried at 150 °C for 30 min in air.

Sample Characterizations. All of the film thicknesses were measured as ~90 nm using a surface profiler (Kosaka ET-3000i), and the film conductivity was obtained using a 4-point-probe measurement (FPP-RS8, Dasol Eng.). The surface morphologies of the films were measured with an AFM (Dimension 3100, Veeco). The investigation of the surface composition was carried out using XPS (AXIS-NOVA, Kratos) equipped with a monochromatized Al Kα source under a high vacuum of 5×10^{-8} Torr. In all XPS spectra, the binding energies were referenced to the C 1s set to 285.0 eV. The Raman spectra of the films were taken using a Jobin Yvon Horiba LabRam HR800 Raman system with a 632.8 nm HeNe laser as an excitation source. For the in-plane conductivity measurements, Ti/Au (5 nm/100 nm) electrodes were deposited onto the cleaned substrates using an e-beam evaporation system. To measure the out-of-plane conductivity, vertical structures with via-hole contacts were fabricated. Ti/Au (5 nm/100 nm) bottom electrodes on the cleaned substrates were deposited, and then, a general photolithography process was carried out twice to pattern the electrodes and make 90 μm square via-holes. After coating each PEDOT:PSS, a Au electrode for the top contact was deposited onto each PEDOT:PSS layer using a shadow mask. The electrical measurements were carried out with semiconductor parameter analyzers (HP4155A) at room temperature. To investigate the bottom surface of the solvent-treated PEDOT:PSS films, we used a lift-off method,[43,44] which can derive the surface energy difference between the substrate and the polymer film, and thus, the films were lifted from the substrate to expose the bottom surface. Each film was immersed in a water bath for 5 min at room temperature and lifted off the glass substrate while maintaining its thin-film shape. The films were transferred onto different glass substrates. Transferred films were baked on a hot plate at 150 °C for 30 min to remove residual solvents for AFM and XPS measurements. The work function of the films was measured by ultraviolet photoelectron spectroscopy (AXIS-NOVA, Kratos) under a base pressure of 5×10^{-8} Torr using He I with an energy of 21.2 eV.

Device Fabrication and Characterization. The modified PEDOT:PSS films were used as transparent anodes in PLEDs and PSCs. The pristine PH 1000 films were spin-coated onto the cleaned glass substrates using a 0.45 μm hydrophilic filter and treated by solvent vapor annealing with DMSO. For reference, the PEDOT:PSS anode was also prepared by adding 5% dimethylsulfoxide (DMSO) to an aqueous solution of PH 1000 before spin-casting. Each PEDOT:PSS anode was subsequently annealed at 150 °C for 30 min.

First, the configuration of the PLEDs was Glass/PEDOT:PSS (90 nm)/F8BT (100 nm)/Ca (20 nm)/Al (100 nm). For fabrication of the emissive layer, 20 mg of F8BT (purchased from American Dye Source) was dissolved in 1 mL of chlorobenzene, and then, the solution was stirred at 50 °C for 10 h in a N_2-filled glovebox. The emissive layers of each device were fabricated by spin-coating onto the modified PEDOT:PSS layers using a 0.45 μm PTFE filter and then annealed at 110 °C for 10 min. Ca/Al were deposited as the top electrodes by thermal evaporation under vacuum at a pressure of 10^{-6} Torr through a shadow mask to produce a device-active area of 4.64 mm^2. The current–voltage–luminescence characteristics of the PLEDs were measured with a Keithley 2400 source measure unit and a Photo Research PR650 spectrophotometer.

Next, the configuration of the PSCs was Glass/PEDOT:PSS (90 nm)/P3HT and PCBM (220 nm)/Ca (20 nm)/Al (100 nm). To form a photoactive layer, a blended solution of 25 mg of P3HT (Rieke Metals) and 25 mg of PCBM (Nano-C) in 1 mL of 1,2-dichlorobenzene was spin-coated on the modified PEDOT:PSS anodes under N_2. Then, a solvent-annealing treatment was performed by keeping the photoactive films inside a covered glass jar for 2 h directly after spin coating, followed by additional thermal-annealing at 110 °C for 10 min. Finally, the cathode consisting of 100 nm Al on top of 20 nm Ca was thermally evaporated through a shadow mask to produce a cell area of 4.64 mm^2 under a vacuum at a pressure of 10^{-6} Torr. The photocurrent density–voltage (J–V) curves were obtained using a Keithley 237 source measurement unit, and the cell performances were measured with and without 100 mW/cm^2 illumination under an AM 1.5 G condition in a N_2-filled glovebox. For accurate measurements, the light intensity was precisely calibrated using a standard silicon solar cell (PVM188 with a KG5 color-filtered window) certified by the NREL.

AUTHOR INFORMATION

Corresponding Author

*E-mail: nsi12@jbnu.ac.kr (S.-I.N.); kimdy@gist.ac.kr (D.-Y.K.).

Notes

The authors declare no competing financial interest.

ACKNOWLEDGMENTS

This work was supported by the Korea Institute of Science and Technology (KIST) Institutional Program, the R & D program funded by Jeollabuk-do, the Ministry of Knowledge Economy (MKE) (Grant No. 2010-H-003-00030100-2010), the National Research Foundation of Korea (NRF) grant funded by the Korea government (MEST) (Grant No. 2011-0029858),

NCRC grant (No.R15-2008-006-02001-0), and the GSR_IC Project through a grant provided by GIST in 2011.

REFERENCES

(1) Yu, G.; Gao, J.; Hummelen, J. C.; Wudl, F.; Heeger, A. J. *Science* **1995**, *270*, 1789−1791.
(2) Burroughes, J. H.; Bradley, D. D. C.; Brown, A. R.; Marks, R. N.; Mackay, K.; Friend, R. H.; Burns, P. L.; Holmes, A. B. *Nature* **1990**, *347*, 539−541.
(3) Norman, K.; Madsen, M. V.; Gevorgyan, S. A.; Krebs, F. C. *J. Am. Chem. Soc.* **2010**, *132*, 16883−16892.
(4) Hecht, D. S.; Hu, L.; Irvin, G. *Adv. Mater.* **2011**, *23*, 1482−1513.
(5) Na, S.-I.; Kim, S.-S.; Jo, J.; Kim, D.-Y. *Adv. Mater.* **2008**, *20*, 4061−4067.
(6) Fehse, K.; Walzer, K.; Leo, K.; Lövenich, W.; Elschner, A. *Adv. Mater.* **2007**, *19*, 441−444.
(7) Zhang, F.; Johansson, M.; Andersson, M. R.; Hummelen, J. C.; Inganäs, O. *Adv. Mater.* **2002**, *14*, 662−665.
(8) Lee, J.-Y.; Connor, S. T.; Cui, Y.; Peumans, P. *Nano Lett.* **2008**, *8*, 689−692.
(9) Wu, Z.; Chen, Z.; Du, X.; Logan, J. M.; Sippel, J.; Nikolou, M.; Kamaras, K.; Reynolds, J. R.; Tanner, D. B.; Hebard, A. F.; Rinzler, A. G. *Science* **2004**, *305*, 1273−1276.
(10) Rowell, M. W.; Topinka, M. A.; McGehee, M. D.; Prall, H.-J.; Dennler, G.; Sariciftci, N. S.; Hu, L.; Gruner, G. *Appl. Phys. Lett.* **2009**, *88*, 233506.
(11) Kim, K. S.; Zhao, Y.; Jang, H.; Lee, S. Y.; Kim, J. M.; Kim, K. S.; Ahn, J.-H.; Kim, P.; Choi, J.-Y.; Hong, B. H. *Nature* **2009**, *457*, 706−710.
(12) Jo, G.; Na, S.-I.; Oh, S.-H.; Lee, S.; Kim, T.-S.; Wang, G.; Choe, M.; Park, W.; Yoon, J.; Kim, D.-Y.; Kahng, Y. H.; Lee, T. *Appl. Phys. Lett.* **2010**, *97*, 213301.
(13) Kirchmeyer, S.; Reuter, K. *J. Mater. Chem.* **2005**, *15*, 2077−2088.
(14) Groenendaal, L.; Jonas, F.; Freitag, D.; Pielartzik, H.; Reynolds, J. R. *Adv. Mater.* **2000**, *12*, 481−494.
(15) Nardes, A. M.; Kemerink, M.; Janssen, R. A. J.; Bastiaansen, J. A. M.; Kiggen, N. M. M.; Langeveld, B. M. W.; van Breemen, A. J. J. M.; de Kok, M. M. *Adv. Mater.* **2007**, *19*, 1196−1200.
(16) Lang, U.; Müller, E.; Naujoks, N.; Dual, J. *Adv. Funct. Mater.* **2009**, *19*, 1215−1220.
(17) Jönsson, S. K. M.; Birgerson, J.; Crispin, X.; Greczynski, G.; Osikowicz, W.; Denier van der Gon, A. W.; Salaneck, W. R.; Fahlman, M. *Synth. Met.* **2003**, *139*, 1−10.
(18) Nardes, A. M.; Janssen, R. A. J.; Kemerink, M. A. *Adv. Funct. Mater.* **2008**, *18*, 865−871.
(19) Na, S.-I.; Wang, G.; Kim, S.-S.; Kim, T.-W.; Oh, S.-H.; Yu, B.-K.; Lee, T.; Kim, D.-Y. *J. Mater. Chem.* **2009**, *19*, 9045−9053.
(20) Crispin, X.; Jakobsson, F. L. E.; Crispin, A.; Grim, P. C. M.; Andersson, P.; Volodin, A.; van Haesendonck, C.; Van der Auweraer, M.; Salaneck, W. R.; Berggren, M. *Chem. Mater.* **2006**, *18*, 4354−4360.
(21) Quyang, J.; Xu, Q.; Chu, C.-W.; Yang, Y.; Li, G.; Shinar, J. *Polymer* **2004**, *45*, 8443−8450.
(22) Ouyang, J.; Chu, C.-W.; Chen, F.-C.; Xu, Q.; Yang, Y. *Adv. Funct. Mater.* **2005**, *15*, 203−208.
(23) Aernouts, T.; Vanlaeke, P.; Geens, W.; Poortmans, J.; Heremans, P.; Borghs, S.; Mertens, R.; Andriessen, R.; Leenders, L. *Thin Solid Films* **2004**, *451*−*452*, 22−25.
(24) Yoo, J. E.; Lee, K. S.; Garcia, A.; Tarver, J.; Gomez, E. D.; Baldwin, K.; Sun, Y.; Meng, H.; Nguyen, T.-Q.; Loo, Y.-L. *Proc. Natl. Acad. Sci. U.S.A.* **2010**, *107*, 5712−5717.
(25) Zhou, Y.; Cheun, H.; Choi, S.; Potscavage, W. J.; Fuentes-Hernandez, C.; Kippelen, B. *Appl. Phys. Lett.* **2010**, *97*, 153304.
(26) Zhou, Y.; Cheun, H.; Choi, S.; Fuentes-Hernandez, C.; Kippelen, B. *Org. Electron.* **2011**, *12*, 827−831.
(27) Kim, Y. H.; Sachse, C.; Machala, M. L.; May, C.; Müller-Meskamp, L.; Leo, K. *Adv. Funct. Mater.* **2011**, *21*, 1076−1081.
(28) Yeo, J.-S.; Yun, J.-M.; Kim, S.-S.; Kim, D.-Y.; Kim, J.; Na, S.-I. *Semicond. Sci. Technol.* **2011**, *26*, 034010.
(29) Do, H.; Reinhard, M.; Vogeler, H.; Puetz, A.; Klein, M. F. G.; Schabel, W.; Colsmann, A.; Lemmer, U. *Thin Solid Films* **2009**, *517*, 5900−5902.
(30) Ma, H.; Yip, H.-L.; Huang, F.; Jen, A. K.-Y. *Adv. Funct. Mater.* **2010**, *20*, 1371−1388.
(31) Na, S.-I.; Kim, T.-S.; Oh, S.-H.; Kim, J.; Kim, S.-S.; Kim, D.-Y. *Appl. Phys. Lett.* **2010**, *97*, 223305.
(32) Lee, T.-W.; Chung, Y. *Adv. Funct. Mater.* **2008**, *18*, 2246−2252.
(33) Nardes, A. M.; Kemerink, M.; de Kok, M. M.; Vinken, E.; Maturova, K.; Janssen, R. A. J. *Org. Electron.* **2008**, *9*, 727−734.
(34) Mäkinen, A. J.; Hill, I. G.; Shashidhar, R.; Nikolov, N.; Kafafi, Z. H. *Appl. Phys. Lett.* **2001**, *79*, 557.
(35) Sun, X. H.; Cheng, L. F; Liu, M. W.; Liao, L. S.; Wong, N. B.; Lee, C. S.; Lee, S. T. *Chem. Phys. Lett.* **2003**, *370*, 425−430.
(36) Helander, M. G.; Wang, Z. B.; Qiu, J.; Greiner, M. T.; Puzzo, D. P.; Liu, Z. W.; Lu, Z. H. *Science* **2011**, *332*, 944−947.
(37) Steim, R. F.; Kogler, R.; Brabec, C. J. *J. Mater. Chem.* **2010**, *20*, 2499−2512.
(38) Yun, J.-M.; Yeo, J.-S.; Kim, J.; Jeong, H.-G.; Kim, D.-Y.; Noh, Y.-J.; Kim, S.-S.; Ku, B.-C.; Na, S.-I. *Adv. Mater.* **2011**, *23*, 4923−4928.
(39) Dickey, K. C.; Anthony, J. E.; Loo, Y.-L. *Adv. Mater.* **2006**, *18*, 1721−1726.
(40) Lee, W. H.; Kim, D. H.; Cho, J. H.; Jang, Y.; Lim, J. A.; Kwak, D.; Cho, K. *Appl. Phys. Lett.* **2007**, *91*, 092105.
(41) Huang, J.; Miller, P. F.; Wilson, J. S.; de Mello, A. J.; de Mello, J. C.; Bradley, D. D. C. *Adv. Funct. Mater.* **2005**, *15*, 290−296.
(42) Zotti, G.; Zecchin, S.; Schiavon, G.; Louwet, F.; Groenendaal, L.; Crispin, X.; Osikowicz, W.; Salaneck, W.; Fahlman, M. *Macromolecules* **2003**, *36*, 3337−3344.
(43) Oh, J. Y.; Jang, W. S.; Lee, T. I.; Myoung, J.-M.; Baik, H. K. *Appl. Phys. Lett.* **2011**, *98*, 023303.
(44) Xu, Z.; Chen, L.-M.; Yang, G.; Huang, C.-H.; Hou, J.; Wu, Y.; Li, G.; Hsu, C.-S.; Yang, Y. *Adv. Funct. Mater.* **2009**, *19*, 1227−1234.
(45) Kim, J. Y.; Jung, J. H.; Lee, D. E.; Joo, J. *Synth. Met.* **2002**, *126*, 311−316.
(46) Jukes, P. C.; Martin, S. J.; Higgins, A. M.; Geoghegan, M.; Jones, R. A. L.; Langridge, S.; Wehrum, A.; Kirchmeyer, S. *Adv. Mater.* **2004**, *16*, 807−811.
(47) Walheim, S.; Böltau, M.; Mlynek, J.; Krausch, G.; Steiner, U. *Macromolecules* **1997**, *30*, 4995−5003.
(48) Yao, Y.; Hou, J.; Xu, Z.; Li, G.; Yang, Y. *Adv. Funct. Mater.* **2008**, *18*, 1783−1789.
(49) Zhou, Y.; Zhang, F.; Tvingstedt, K.; Barrau, S.; Li, F.; Tian, W.; Inganäs, O. *Appl. Phys. Lett.* **2008**, *92*, 233308.
(50) Kim, W. H.; Mäkinen, A. J.; Nikolov, N.; Shashidhar, R.; Kim, H.; Kafafi, Z. H. *Appl. Phys. Lett.* **2002**, *80*, 3844.
(51) Park, J. H.; Park, O O.; Yu, J.-W.; Kim, J. K.; Kim, Y. C. *Appl. Phys. Lett.* **2004**, *84*, 1783.
(52) Chen, L.-M.; Hong, Z.; Li, G.; Yang, Y. *Adv. Mater.* **2009**, *21*, 1434−1449.